

Time series autoregression technique implemented on-line in DIAS system for ionospheric forecast over Europe

K. Koutroumbas, I. Tsagouri, and A. Belehaki

National Observatory of Athens, Institute for Space Applications and Remote Sensing, Greece

Received: 2 February 2007 – Revised: 17 July 2007 – Accepted: 6 November 2007 – Published: 26 February 2008

Abstract. A new method for ionospheric predictions based on time series autoregressive models (*AR*) that was recently developed to serve the needs of the European Digital Upper Atmosphere Server (DIAS) for short term forecast of the *f*o*F*2 parameter over Europe (up to the next 24 h) is described. Its performance for various steps ahead is compared with the outcome of neural network predictors for both storm and quiet periods in two DIAS locations, Athens and Pruhonice. The results indicate that the proposed method provides robust short term forecasts of the *f*o*F*2 for the middle latitude ionosphere.

Keywords. Ionosphere (Ionospheric disturbances; Mid-latitude ionosphere; Modeling and forecasting; Instruments and techniques)

1 Introduction

The accurate prediction of ionospheric conditions especially during periods characterized by solar and geomagnetic disturbances is a strong requirement for the reliable performance of several applications including HF communications and satellite positioning and navigation applications. In particular, the parameters that have received a great deal of attention are the peak *F* region electron density (Nm*F*2) and the related critical frequency (*f*o*F*2), since they are both related to the maximum usable frequency (MUF) for oblique propagation of radio waves, as well as the total electron content (TEC), which is another key parameter related to phase delay effects on the GPS navigation signals (Fuller-Rowell et al., 2000a).

Long-term ionospheric predictions are generally based upon predictions of driving parameters such as the sunspot number, the 10.7 cm solar flux, and magnetic activity indices.

Correspondence to: K. Koutroumbas
(koutroum@space.noa.gr)

Unfortunately these parameters are not easy to predict. In addition, the functions relating these parameters with the ionosphere are imprecise. Therefore, long term predictions are subject to a considerable amount of uncertainty even in the medians. Short-term ionospheric predictions (or forecasts) generally refer to departures from the median behavior. The short-term fluctuations may be specified in terms of hour-to-hour, day-to-day, and week-to-week variabilities. There are also second-to-second and minute-to-minute variations but this class of variations generally falls within the realm of unpredictable behavior (Goodman, 2005). These very short-term forecasts are generally referred to as nowcasts. Ionospheric predictions in the short and intermediate term provide the most exciting challenge for the ionospheric researchers.

Ionospheric predictions are mainly based on ionospheric modeling that assumes a number of forms ranging from the purely theoretical to the totally empirical. Although theoretical models (e.g., Crowley et al., 1996; Daniell et al., 1995) could be considered as powerful tools for physical analyses providing real input in the understanding of the mechanisms that govern the ionospheric formation under various geophysical conditions, they hardly offer real contribution in operational applications (Mikhailov et al., 2007). On the other hand, the empirical approach based on the correlation between the ionospheric disturbances and the level of the geomagnetic activity as it is described by various geomagnetic activity indices (Fuller-Rowell et al., 2000b; Fuller-Rowell et al., 2002; Kutiev and Muhtarov, 2001 a, b, 2003; Muhtarov and Kutiev, 1999; Muhtarov et al., 2002; Tsagouri and Belehaki, 2006), is widely used in practice. Besides the operational implementation, the empirical modelling exhibits certain advantages compared to the theoretical modelling if a good data set is available. The main advantage of the empirical models is that their analytical expressions are fitted to the data, so there is no systematic deviation (offset) between the model and data. However, the main problem of empirical models is how well their analytical expressions describe the

observed variations (Kutiev and Muhtarov, 2003). Moreover the utilization of geomagnetic indices to ionospheric prediction models may cause a number of complications that arise from the following two facts a) geomagnetic indices do not provide high enough correlation with the relative $foF2$ deviation from monthly medians (Mikhailov et al., 2007); b) the only geomagnetic index which is available for real-time use is the predicted daily Ap index. The accuracy of the geomagnetic index predictability is an issue of major consideration. In addition, the transformation of the daily Ap to an hourly index would impose additional uncertainty in the forecasting models.

To overcome these problems, an alternative approach is provided by the real-time ionospheric models that are used for ionospheric specification and short term prediction of the absolute value of the ionospheric parameters and are supported mainly by time series forecasting techniques. Data-driven modelling techniques of this kind are the standard auto-correlation and autocovariance prediction models. In addition, neural network models have also been used in this framework. Their utilization is based on the assumption that ionospheric variability is dominated by non linear processes (e.g. Koutroumbas and Belehaki, 2005; Tulunay et al., 2004a, b; Cander, 2003; Stanislawska and Zbyszynski, 2001; McKinnell and Poole, 2001; Wintoft and Cander, 2000a, b). In the utmost case only previous observations of the predicted parameter are used for training the adopted model. By using these techniques, one can obtain predictions of the hourly values of the ionospheric $F2$ layer critical frequency, $foF2$, up to 24 h ahead. Statistical studies suggest that time series forecasting techniques usually provide very useful tools for reliable predictions under relatively quiet or moderate geomagnetic conditions, but they have been proved inadequate under intensively disturbed geomagnetic conditions (Cander, 2003; Stanislawska and Zbyszynski, 2002). The results reveal a general problem related to any statistical approach: intense or great storms are rare events and practically they are not included in the training period when it is relatively short. On the other hand, when the training period is long the effects of such outstanding events are just lost in the sea of quiet time and slightly disturbed conditions after a statistical treatment (Mikhailov et al., 2007).

The field of ionospheric predictions is undergoing continuous evolution with the introduction of new scientific methods and instruments. The requirement for quasi-real-time products based upon current ionospheric specification has led to an increased importance of so-called real-time ionospheric models. Ionospheric specification tools comprise terrestrial sounding systems, including real-time networks of ionospheric sounders (Galkin et al., 2006). The European Digital Upper Atmosphere Server – DIAS (Belehaki et al., 2005; 2006) is based on the European real-time network of ionosondes and has as primary objective to cover the needs of the operational applications for reliable information on the current conditions of the ionosphere over Europe and for ac-

curate forecasting information in long term and short term time scales (<http://www.iono.noa.gr/DIAS>). To achieve this goal, DIAS designed and developed a full range of ionospheric products, such as real-time ionograms with the automatic scaling results, frequency plots of ionospheric parameters important for radio propagation, maps of $foF2$, $M(3000)F2$, MUF and electron density for specification, long term prediction and short term forecast, as well as alerts and warnings for forthcoming ionospheric disturbances. In order to deliver those products, DIAS developed a pan-European digital data collection, based on real-time information as well as historical data provided by most of the operating ionospheric stations in Europe. DIAS has already started its operation in August 2006, and the delivered products and services are available in the address <http://dias.space.noa.gr>.

The aim of this paper is to present a new method for short term ionospheric forecast up to 24 h ahead, based on the autoregression models. To assess the performance of the method we compare the results with those obtained from a similar method that employs neural network models. The proposed method is currently used by the DIAS system and delivers forecasts of the $foF2$ parameter for up to the next 24 h, for several middle latitude locations in Europe where DIAS ionospheric stations operate.

In Sect. 2 we present a description of the proposed method and in Sect. 3 the method's performance is assessed under storm and quiet conditions using data from Athens (38° N, 23.5° E) and Pruhonice (50° N, 14.6° E) digisondes. In addition, this section includes a comparison of the above results with those obtained by using the neural network (NN) based method. Finally in the last section we summarize our conclusions.

2 Proposed method

In this paper we deal with the problem of forecasting $foF2$. More specifically, based on its current as well as its previous M values, the aim is to forecast $foF2$ s steps ahead (in our case $s=1$ for 15 min, $s=4$ for 1 h, $s=8$ for 2 h, ..., $s=96$ for 24 h) using autoregressive (AR) modeling. Focusing on a specific value of s at the beginning of a calendar month, the data of the previous calendar month are used to estimate the AR model that will be used for the estimation of $foF2$ for the current calendar month. More precisely, various AR models are tested on the above data of the previous calendar month and the best one (according to the mean square error criterion) is adopted.

Before we state explicitly the proposed method, a short description of AR models is in order.

2.1 Basics of AR modeling

Consider a stochastic process $\{x(n)\}$. The problem of interest is the estimation of the value of the process s

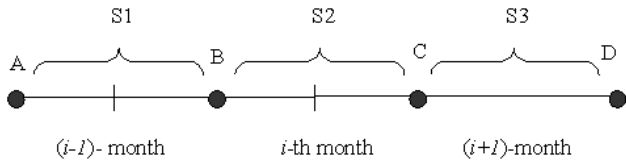


Fig. 1. At each epoch AR models are re-estimated based on the measurements of the previous month.

steps ahead. More specifically, we would like to estimate the value $x(n + s)$ based on the set of values $T = \{x(n), x(n-1), \dots, x(n-M)\}$. Assuming that the process at hand is described by an AR model, the minimum mean square error (MMSE) linear estimator of $x(n+s)$, denoted by $\hat{x}(n+s)$, is given by

$$\hat{x}(n+s) = w_0 x(n) + w_1 x(n-1) + \dots + w_M x(n-M) = \mathbf{w}^T \cdot \mathbf{x}_n, \quad (1)$$

where M is the order of the AR model, $\mathbf{w} = [w_0, w_1, \dots, w_M]^T$ is its parameter vector (see Kalouptsidis, 1997) and $\mathbf{x}_n = [x(n), x(n-1), \dots, x(n-M)]^T$. Both M and \mathbf{w} are crucial for the complete determination of an AR model.

Fixing M , the determination of \mathbf{w} is based on a time series

$$Y = \{x(0), x(1), \dots, x(l)\}, \quad (2)$$

of length l , with $l \gg M$. More specifically, it can be shown (see e.g. Kalouptsidis, 1997) that \mathbf{w} is the solution of the following system of linear equations

$$R\mathbf{w} = \mathbf{p}, \quad (3)$$

where

$$R = \begin{bmatrix} r(0) & r(1) & \dots & r(M) \\ r(1) & r(0) & \dots & r(M-1) \\ \vdots & \vdots & \ddots & \vdots \\ r(M) & r(M-1) & \dots & r(0) \end{bmatrix}, \quad (4)$$

$$\mathbf{p} = [r(s), r(s+1), \dots, r(s+M)]^T \quad (5)$$

and $r(i)$ is the i -th lag autocorrelation coefficient, which measures the correlation between two values of the time series that lie at time distance i from each other. $r(i)$ is estimated via the following equation

$$r(i) = \frac{1}{l-i} \sum_{j=1}^{l-i} x(j)x(i+j) \quad (6)$$

¹ T denotes the transpose operator.

²It is assumed that the process under study is ergodic.

2.2 Choice of the best AR model

Clearly, an AR model is completely determined by its order M and its parameter vector \mathbf{w} . In practice, however, the order M of the model that best describes the data is unknown. A simple method for estimating M and the corresponding parameter vector \mathbf{w} of the AR model that best describes the data, using the time series data $S = \{x(0), \dots, x(l), x(l+1), \dots, x(m)\}$, called *Best Model Determination Method (BMDM)*, is given next:

- Divide S into two sets $X_1 = \{x(0), \dots, x(l)\}$ and $X_2 = \{x(l+1), \dots, x(m)\}$.
- For $M=1$ to M_{\max} do
 - Determine w using Eq. (3), adopting X_1 in the place of Y .
 - Estimate the mean square error MSE_M for the above model by using the subset X_2 as

$$\begin{aligned} MSE_M &= \sum_{n=l+1}^{m-s} (x(n+s) - \hat{x}_M(n+s))^2 \\ &= \sum_{n=l+1}^{m-s} (x(n+s) - \mathbf{w}^T \cdot \mathbf{x}_n)^2, \end{aligned} \quad (7)$$

where $\hat{x}_M(n+s) = \mathbf{w}^T \cdot \mathbf{x}_n$ is the linear MMSE estimate of order M computed by Eq. (1), where as parameter vector \mathbf{w} we use the one produced in the previous step.

- End { For }
- Adopt the model with the smallest MSE as the one that best describes the data under study.

2.3 Application to foF2 forecasting

Let us turn our attention now on the specific problem of the estimation of the values of the foF2 parameter. More precisely, taking into account that the sampling rate is 15 min, we would like to have estimates of the foF2 after 15 min ($s=1$), 1hour ($s=4$), 2h ($s=8$), ..., 24h ($s=96$). Thus, we need to estimate 25 AR models denoted by AR₀ (15 min), AR₁ (1h), AR₂ (2h), ..., AR₂₄ (24h).

Based on the systematic variations of the foF2 value, it has been decided to re-estimate the 25 AR models at the beginning of every calendar month, by taking into account the measurements of the previous calendar month. More specifically (see Fig. 1), suppose that we are at time B (the beginning of a new calendar month). At this time the AR _{i} 's, $i=0, \dots, 24$ are re-estimated based on the S_1 time series segment (which corresponds to the previous month). In particular, we divide S_1 in two subsets, X_1 , which contains the data of the first half of the previous month and X_2 , which contains the data of the second half of the previous month, and we apply

the BMDM method described above. Clearly, BMDM will be applied 25 times, one for each AR_i model. At time C (the beginning of the next month), we re-estimate the AR_i 's based on S_2 and so forth. Note that after its estimation, each AR_i is applied every time a new observation becomes available (in our case every 15 min).

3 Performance evaluation

The performance of the proposed method, hereafter denoted by TSAR1 (Time Series AutoRegressive using 1 month data), which is the version running in DIAS system, is compared with predictions obtained using a similar method that, instead of AR models, it uses feedforward neural networks (FNNs) with a single hidden layer (hereafter denoted by TSNN2 (Time Series Neural Network using 2 month data)). In TSNN2, NNs are re-estimated at the beginning of a new month taking into account the previous two calendar months. More specifically, in TSNN2 $X_1 = \{x(0), \dots, x(l)\}$ consists of the observations of the first and a half month and $X_2 = \{x(l+1), \dots, x(m)\}$ consists of the rest observations of the second month. The neural networks used in TSNN take as input the 6 previous values of the $foF2$ (this implies that it has 6 input nodes) and predicts the $foF2$ value s steps ahead (that is it has 1 output node)³. Seven such neural networks are considered at the beginning of each month, for each prediction step, with 2, 4, 6, 8, 10, 12, 14 nodes in the hidden layer⁴ and the one that exhibits the lowest mean square error over the test set is adopted. The above NNs use as training set the $X_1' = \{([x(0), \dots, x(5)]^T, x(6)), ([x(1), \dots, x(6)]^T, x(3)), \dots, ([x(l-6), \dots, x(l-1)]^T, x(l))\}$ and as test set $X_2' = \{([x(l+1), \dots, x(l+6)]^T, x(l+7)), ([x(l+2), \dots, x(l+7)]^T, x(l+8)), \dots, ([x(m-6), \dots, x(m-1)]^T, x(m))\}$. Both TSAR1 and TSNN2 methods share the same general philosophy in the sense that each one of them picks the best model (AR and FNN, respectively), among a set of available models. In the first method, the set of AR models is obtained by varying the order M of the AR model, while in the second method the set of the single hidden layer FNN models is obtained by varying the number of nodes in the hidden layer. However, the TSNN2 uses two months of data for training and testing. This led us, for reasons of thoroughness, to consider also in our comparison the TSAR2 method, which is the same as TSAR1 except that for the estimation of the new AR model at the beginning of each month, the data of the last two calendar months are taken into account. Besides their similarities, TSAR and TSNN differ significantly in the modelling approach: TSAR adopts linear models for the prediction of the absolute $foF2$ values, while TSNN uses non linear models

for the same reason. For clarity reasons, we remind that in TSAR1 and TSAR2, the number of the past values of $foF2$ that are used for prediction is specified by the order M of the corresponding AR model.

Before we proceed, it is important to remind that the main aim of the present paper is to evaluate the performance of the proposed TSAR methods during both geomagnetically quiet intervals and storms. For comparison purposes we also consider the performance of TSNN method. The methods' performance was first investigated during the occurrence of geomagnetic storms. The Dst index was selected as geomagnetic storm indicator since it "monitors" the storm development, assess its intensity and identifies two or three storm phases that correspond to different physical processes. Moreover, besides the well established dependence of the ionospheric storm-time response on the season and the local time of the storm onset in conjunction with the local time and the latitude of the observation point, there is strong evidence for the correlation of the storm development conditions, which are controlled by the IMF and are reflected in the Dst development pattern, with the qualitative signature of ionospheric storm disturbances at middle latitudes (Belehaki and Tsagouri, 2002).

Four storm events of moderate to intense intensity occurred in the following time intervals: 28 August 2004–5 September 2004 (first storm event), 21–31 January 2004 (second storm event), 2–5 April 2004 (third storm event) and 5–9 April 2004 (fourth storm event) are considered here. The geomagnetic conditions in the one and two calendar month periods before each storm event (which were used for the training of TSAR1 and TSAR2, TSNN2 respectively) could be described as follows: for the case of the first storm event, June 2004 is characterized by very low geomagnetic activity, while in July 2004 four disturbed periods were recorded in the second half of the month. The first one was of moderate activity (min Dst ~ 80 nT), while for the rest three successive storm disturbances the Dst index reached a minimum value of about -197 nT. During August 2004, a storm event is recorded at the end of the month, which is the one under study. Here it is important to clarify that the methods' predictions for this storm event were based on the models' estimation by using observations of July (for TSAR1) and June–July (for TSAR2 and TSNN2) for the storm days in August and of August (for TSAR1) and July–August (for TSAR2 and TSNN2) for the storm days in September 2004. Regarding the second storm, during the preceding month (December 2003) geomagnetic activity of very low intensity was recorded, while a great geomagnetic storm (min Dst ~ -422 nT) occurred in November 2003. In the case of the third and forth storm events under study, both the two months prior to the storms (February and March 2004) were in general characterized by low geomagnetic activity.

Ionospheric data from Athens (38.0° N, 23.5° E) and Pruhonice (50.0° N, 14.6° E) of 15 min sampling rate are used to evaluate the performance of the method at middle

³ The reasoning for choosing the 6 most recent values for the s -steps ahead prediction can be found in Koutroumbas and Belehaki (2005).

⁴ For more nodes in the hidden layer no significant differences were encountered.

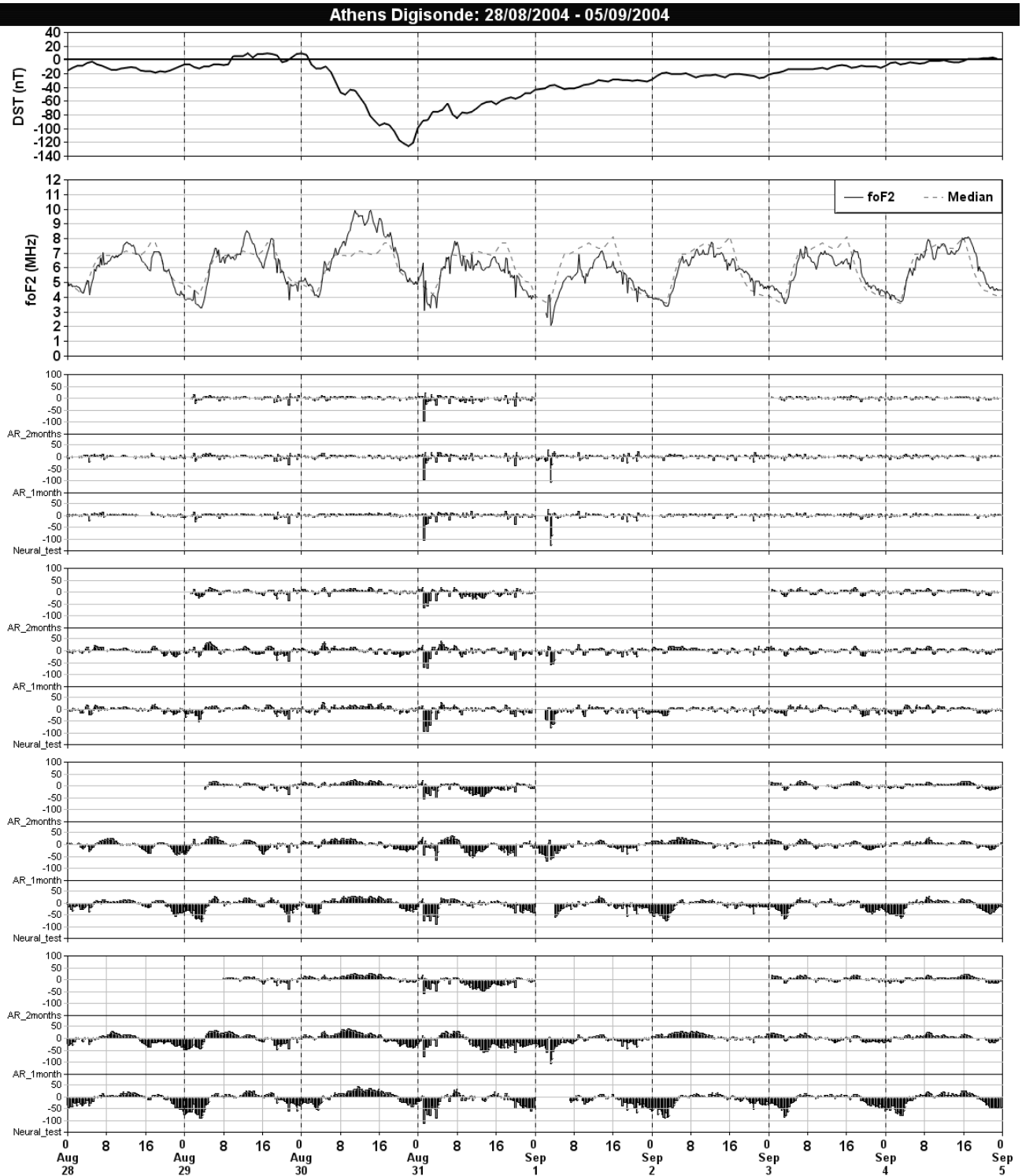


Fig. 2. The Dst index is presented in the top panel followed by the observed $foF2$ parameter from Athens Digisonde and its monthly median value (dashed line), for the storm interval 28 August–4 September 2004. The prediction error parameter is presented in the last four panels for 15 min, 1hr, 3 h and 6 h prediction window. In each panel the prediction error is calculated using the results of the three models under discussion, TSAR2, TSAR1 and TSNN2.

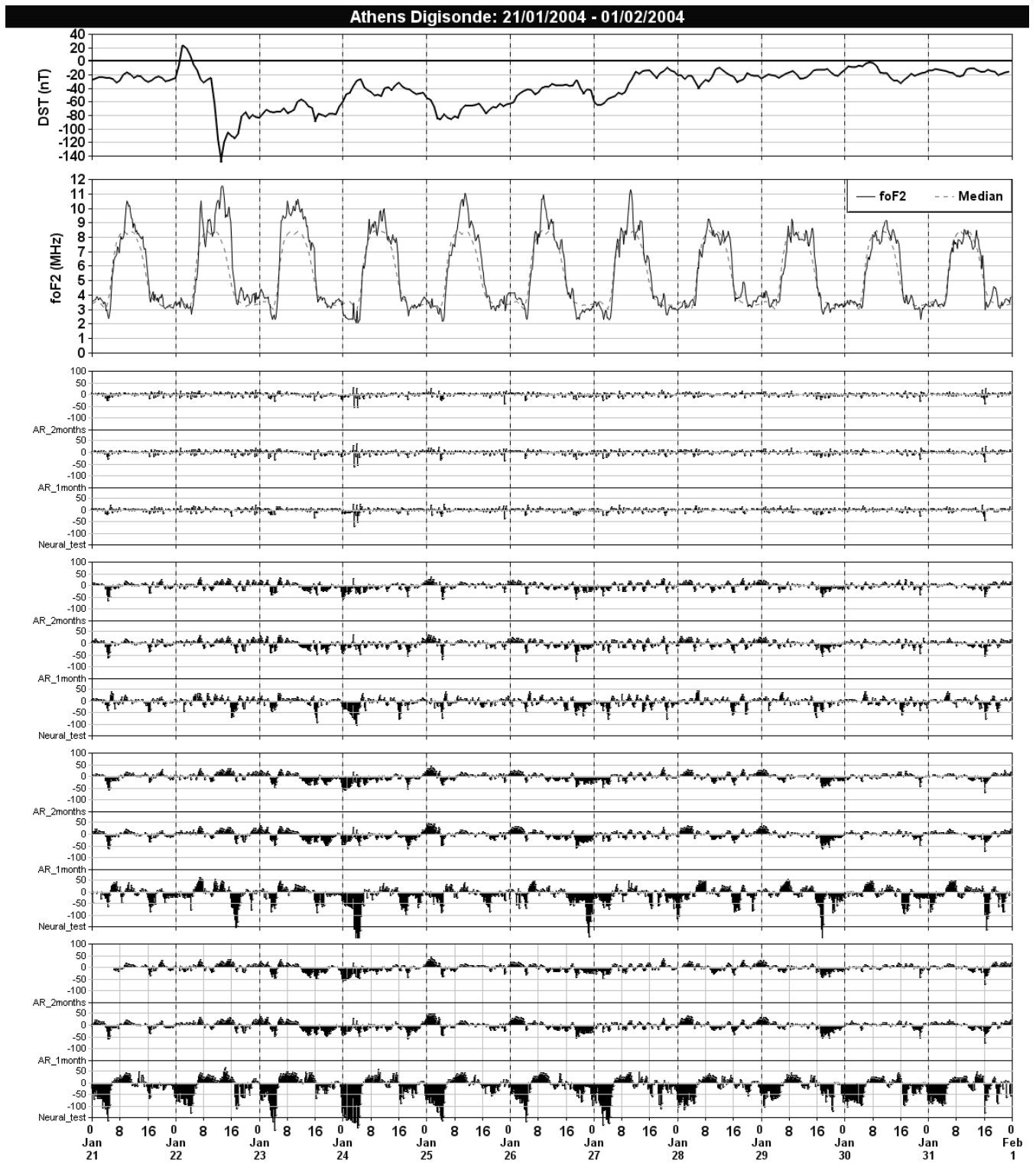


Fig. 3. The same as Fig. 2 for the storm interval 21–31 January 2004.

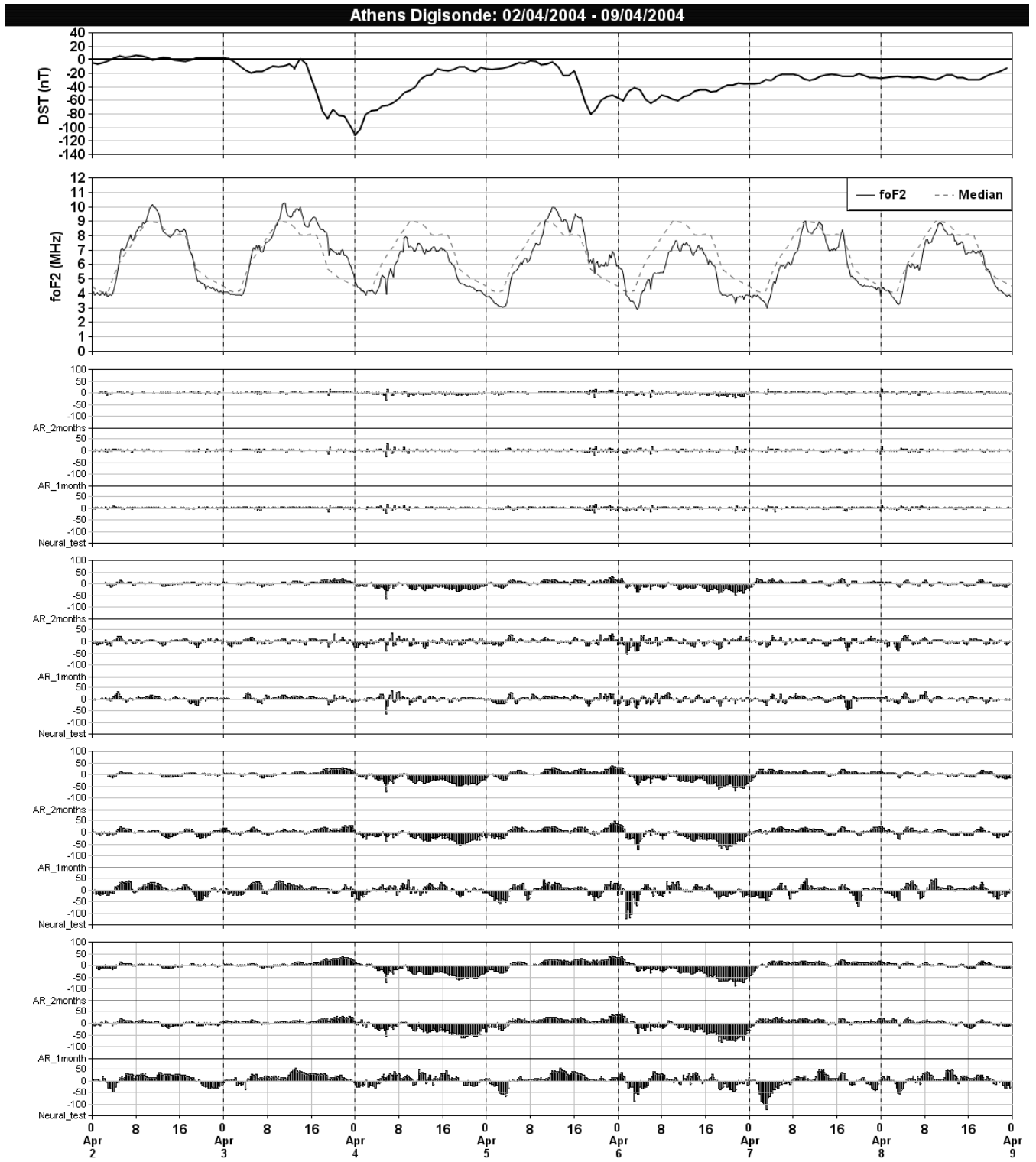


Fig. 4. The same as Fig. 2 for the storm interval 2–8 April 2004.

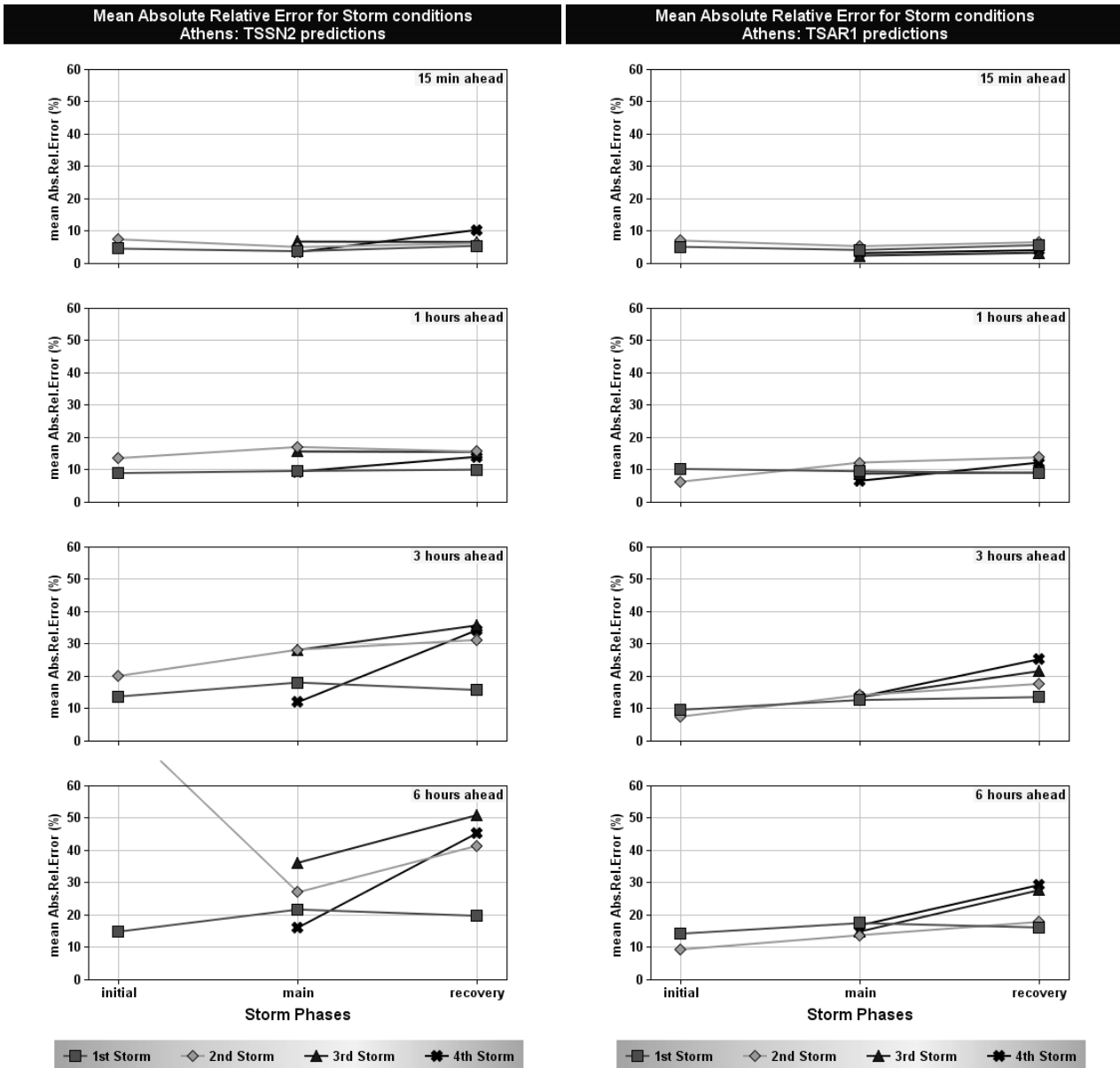


Fig. 5. The mean absolute relative error values for Athens location and for prediction windows 15 min, 1 h, 3 h and 6 h calculated over the three phases of each storm (initial, main and recovery) using the prediction results of the three methods TSSN2 (left column), TSAR1 (right column), TSAR2 (continued in the next page).

latitudes. Concerning the time step of the data sampling, one can argue that since the large scale ionospheric disturbances have a time scale from several hours to one or two days, the 15-min time step used here may be considered to be too small, introducing variations of smaller time scales, which may affect the prediction efficiency of the proposed method. However, the TSAR method was developed to serve not only the delivery of reliable ionospheric forecasts some hours ahead, but also interpolation purposes for the development of reliable near real-time products and services of ionospheric specification within DIAS system. For these pur-

poses, the availability of predictions 15 min and 1 h ahead is a strong requirement and therefore the usage of 15 min sampling rate becomes a necessity. In addition, preliminary tests performed with our time series sampled every hour, gave no significantly different results than the 15 min sample rate case. For the same reason, the predictions of 15 min and 1 h ahead are evaluated next, although they can hardly demonstrate the merits of a method, since the characteristic e-fold time of NmF2 variations is greater than 1.5 h (Mikhailov et al., 2007).

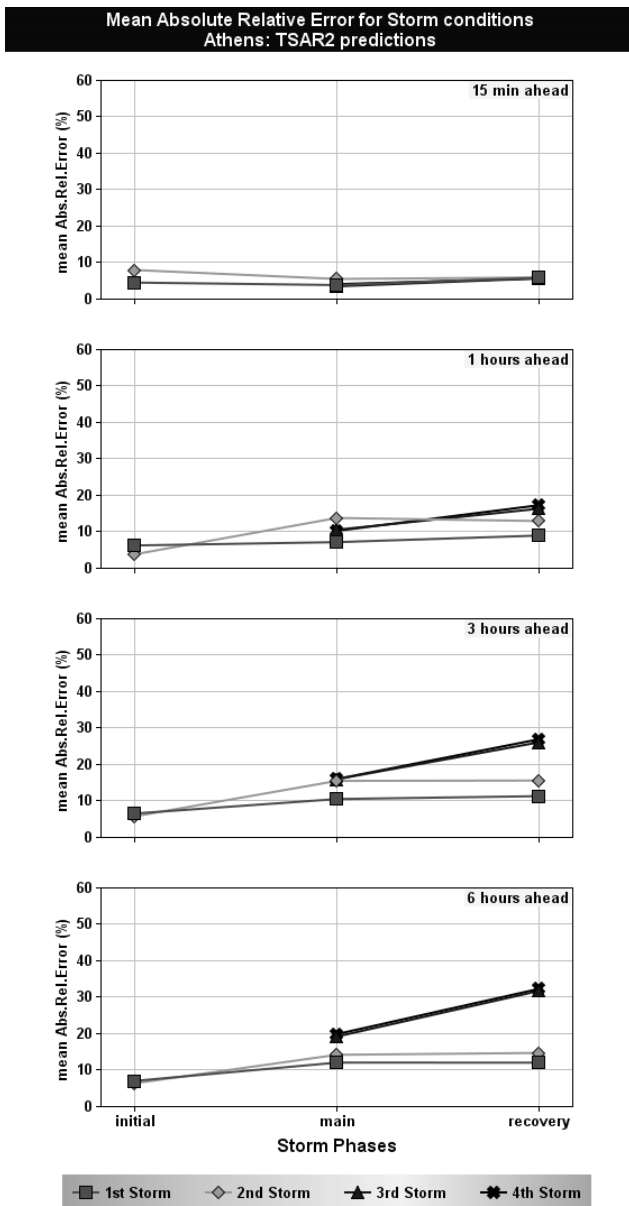


Fig. 5. Continued.

The development characteristics of the Dst index reflect the different conditions of magnetospheric – ionospheric coupling occurred for each storm, which result to different ionospheric storm pattern over Athens. The storm conditions for each of the selected interval are presented in Figs. 2, 3 and 4, where the Kyoto Dst index is presented in the top panel followed by the observed f_oF2 parameter from Athens Digisonde and its monthly median value (dashed line). The performance of the ionospheric methods during the storm events is evaluated using the prediction error parameter defined as:

$$\text{error} = \frac{f_oF2_{\text{obs}} - f_oF2_{\text{mod}}}{f_oF2_{\text{obs}}} \times 100 \quad (8)$$

where f_oF2_{obs} is the observed value of the f_oF2 parameter, computed in real-time with the automatic scaling software ARTIST and f_oF2_{mod} is the forecasted f_oF2 value extracted from the model. The error parameter is presented in the last four panels of Figs. 2–4 for 15 min, 1hr, 3 h and 6 h prediction window. In each panel the prediction error is calculated using the results of all three methods under discussion, TSAR2, TSAR1 and TSNN2.

According to the Dst index the first storm event (Fig. 2) is characterized by an initial phase, followed by a gradually evolving main phase and a slowing recovery lasted for several days. Positive storm effects of short duration recorded during the initial phase, positive storm effects of long duration during the main phase and negative storm effects recorded during the recovery phase, formulate the ionospheric response over Athens during this storm event. The performance of all three methods TSAR1, TSAR2 and TSNN2 present the same qualitative characteristics during the initial and the main phase of the storm, tending to overestimate f_oF2 during the night, and to underestimate it during the day. However, the prediction pattern of TSAR1 and TSAR2 differs significantly from the prediction pattern of TSNN2 during the next days of the recovery phase of the storm when negative effects are recorded over Athens: TSNN2 systematically overestimates the f_oF2 forecasts at night, especially for predictions 3 and 6 h ahead. On the contrary during the day, where negative effects are recorded, TSNN2 gives successful predictions.

The second storm event (Fig. 3) is also characterized by an initial phase, followed by a rapidly evolving main phase and a long lasting recovery phase during which the Dst index presents several excursions. With Athens being in the morning sector during the storm onset, the ionospheric response over Athens is characterized by positive storm effects of long duration during the whole period. All methods' predictions present in general the same qualitative characteristics during the initial and the main phases of the storm, while the pattern of TSNN2 predictions differentiates systematically from the other two during the recovery phase, although positive storm effects are still recorded over Athens. Once again TSNN2 systematically overestimates the f_oF2 forecasts at night, especially for predictions 3 and 6 h ahead. Another point of interest is that the prediction errors are significantly higher in the case of the TSNN2 method. It is noteworthy that for ionospheric forecasts 3 and 6 h ahead this deviation exceeded the 100% during the night, when no significant ionospheric disturbances are recorded. This may be considered as evidence that the TSNN2 predictions suffers from systematic offsets, which are not correlated to the ionospheric storm-time response neither in terms of negative or positive storm effects occurrence nor in terms of ionospheric storm effects' intensity.

The last presented time interval concerns two successive storm events (the third and the fourth storm events described above) and this point is of special interest, since in such cases

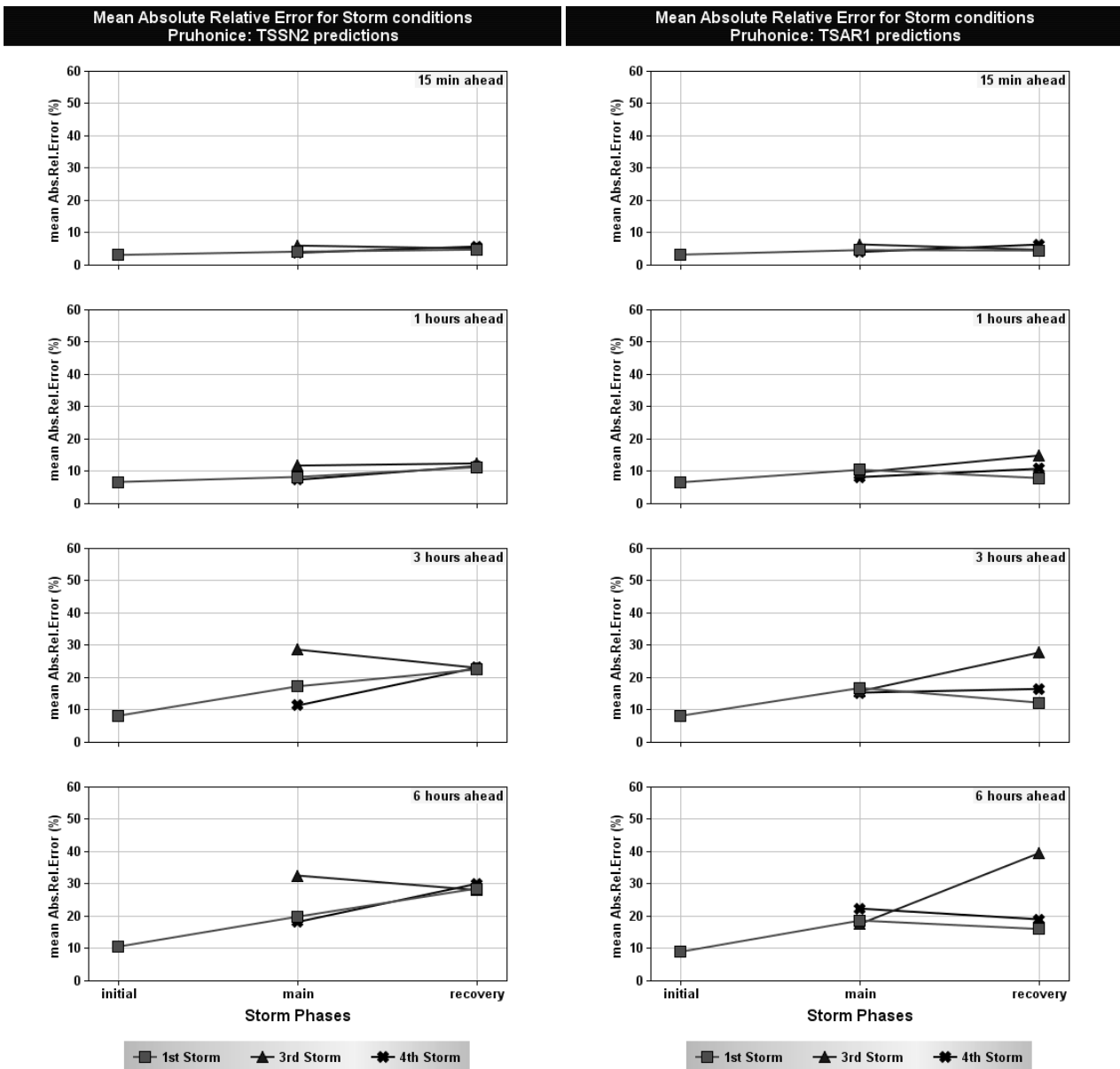


Fig. 6. The same as Fig. 5 for Pruhonice location.

the ionospheric response could be very complicated. The predictions obtained by the three above methods (TSAR1, TSAR2 and TSNN2) for the two storm events are given in Fig. 4. No initial phase is identified for these storms, while the main phase is characterized by a rather gradual development. The first storm recovers within 30 h while the recovery phase of the second one is much more gradual. Positive effects during the first day and negative during the second day of each storm formulate the ionospheric response over Athens. Once again, the performance of TSAR1 and TSAR2, exhibits in general a different pattern in comparison to the performance of TSNN2. The latter tends to give higher val-

ues for $foF2$ during early morning hours and lower $foF2$ values during the day for the whole period, when the prediction pattern of TSAR1 and TSAR2 differs for positive and negative ionospheric storm time response, giving more evidence for the existence of systematic offsets in TSNN2 predictions and for more robust predictions of TSAR1 and TSAR2 methods.

In general, the comparison between the three methods gives evidence for consistency between TSAR1 and TSAR2 predictions, in that the two methods give qualitatively similar results in all cases. In particular, AR models seem more sensitive in capturing successive changes from positive to

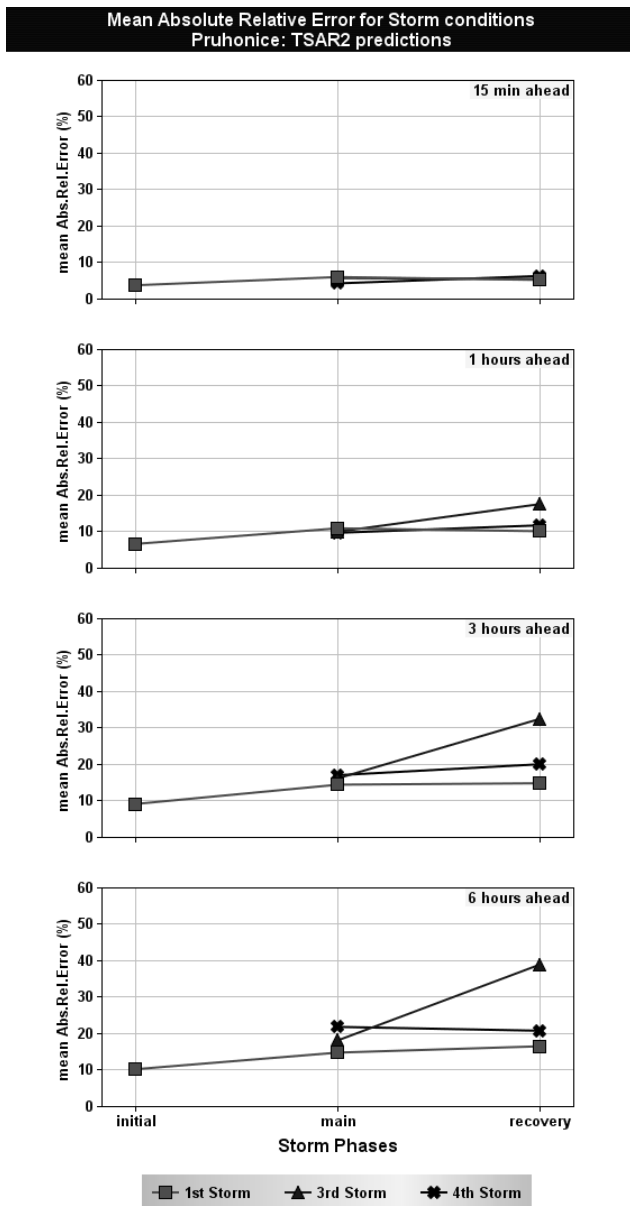


Fig. 6. Continued.

negative (and vice versa) ionospheric storm phases. This is in contrast to the prediction pattern of TSNN2 which is described by the same qualitative characteristics during the whole of a geomagnetically disturbed period independently of the ionospheric activity pattern. The above indicates first that TSAR1 and TSAR2 methods are more capable in capturing successive ionospheric changes, and then that TSNN2 predictions are more affected from the current ionospheric conditions, which seems to introduce systematic offsets in the methods' performance.

In an effort to better organize the results and to quantify the relative performance of the three methods, the mean absolute relative errors over the three phases of each storm (ini-

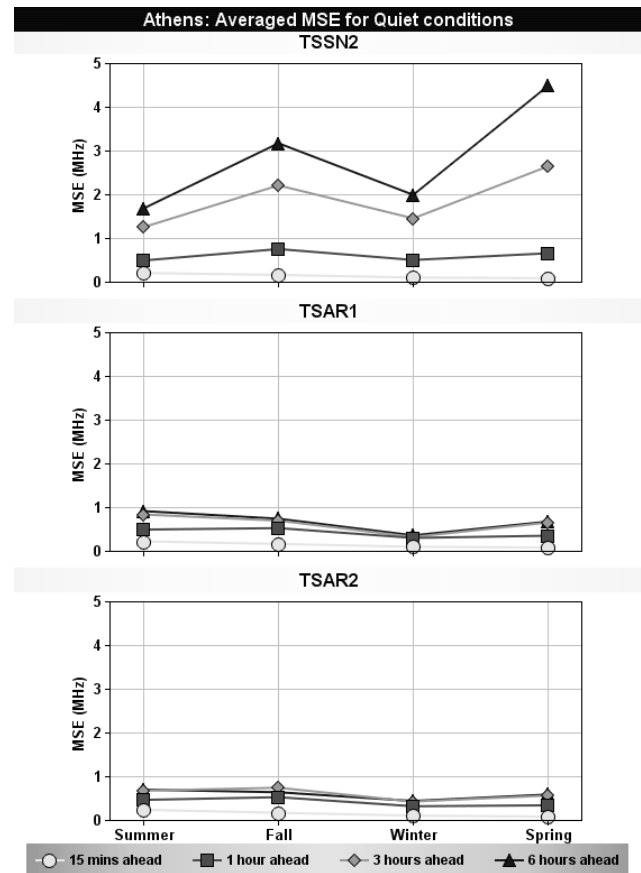


Fig. 7. The average values of the MSE over each season for the quiet intervals listed in Table 1, using the prediction results of the three models TSSN2 (top), TSAR2 (middle), TSAR1 (bottom) for Athens location, for prediction windows 1 h, 3 h and 6 h.

tial, main and recovery) were calculated for all storm events and are presented in Fig. 5 for Athens location. The absolute relative error is defined as the absolute value of the prediction error as defined in Eq. (8). The first remark from the inspection of these results is that the prediction efficiency of all methods becomes poorer for longer prediction time horizon (up to six hours). In addition, the poorer performance of TSNN2 method with respect to both TSAR1 and TSAR2 for a prediction horizon greater than 1 h, is clearly demonstrated with the statistical analysis shown in Fig. 5. An interesting point is that the three methods' provide us with quantitatively comparable results in the case of the first storm event, which is characterized by gradually evolving phases. For the rest three storm periods, which are characterized either by rapid changes in the magnetospheric-ionospheric coupling or by long lasting disturbances, the TSNN2 prediction errors are significantly greater than the prediction errors of TSAR1 and TSAR2. This seems to confirm the argument that TSNN2 performance is not very capable in capturing rapid changes in ionospheric response resulting by fast changing geospace

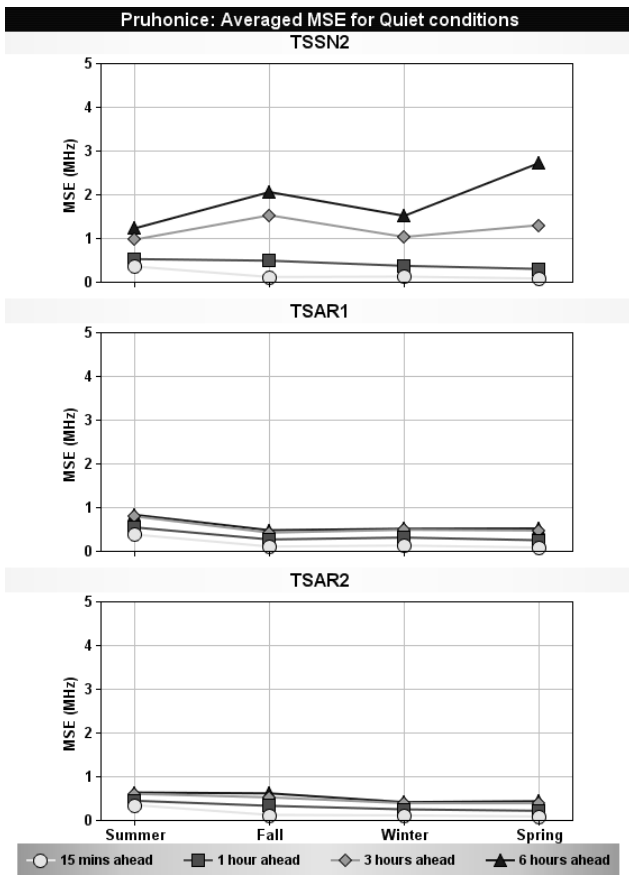


Fig. 8. The same as Fig. 7 for Pruhonice location.

environment conditions. Moreover, TSNN2 predictions are more affected by the recent ionospheric conditions and when an ionospheric disturbance is in progress, systematic deviations are reproduced in the models' estimations.

The mean absolute relative error for the predictions resulted from the TSAR1 and TSAR2 methods, presents comparable values in all cases, sometimes in favor of TSAR1 and sometimes in favor of TSAR2. Here, it is worth comment on the methods' performance during the last two successive storm events. The TSAR1 gives systematically better results compared to TSAR2 in both main and recovery phases, indicating a more direct response of the TSAR1 to successive and rapid changes of the ionospheric conditions. The opposite result is observed for the case of the first storm, where the TSAR2 gives in general better predictions. However, despite the differences once again the comparison between the two methods gives evidence for consistency in their predictions, since the response of the two methods is described by comparable quantitative characteristics. In respect to the storm development, the mean absolute relative error is rather small during the initial phase of the storm, with a general tendency to increase as the storm evolves and recovers. This is rather expected since the methods' predictions are based on

Table 1. List of the geomagnetically quiet intervals used for the evaluation of the proposed method.

Season	Geomagnetically quiet intervals
Summer	1–12 June 2004
	1–14 July 2004
	1–20 August 2005
Fall	1–30 October 2005
Winter	1–31 January 2006
	1–28 February 2006
Spring	1–31 March 2005

the most recent measurements, which progressively include more and more disturbed data as we move to the end of the storm.

In an effort to investigate the validity of the results in other DIAS locations, the mean absolute relative error over the three phases of each storm, was also calculated for three of the storm events under study (the first, the third and the fourth one) for Pruhonice location and is presented in Fig. 6. For the second storm event, *f*oF2 observations for Pruhonice station were no available. The main trends of the TSAR1 and TSAR2 prediction pattern obtained for Athens location are also present in the prediction pattern obtained for Pruhonice location although milder now, showing consistency between the two methods for this location too. In quantitative perspective, the relative errors for Pruhonice are in general slightly greater than the corresponding ones obtained for Athens. The most interesting point is that TSNN2 provides better predictions over Pruhonice than over Athens.

The method predictions were further evaluated during several geomagnetically quiet time intervals listed in Table 1. The average values of the MSE over each season are presented in Fig. 7 for Athens location and in Fig. 8 for Pruhonice location. It is very interesting to note the significant difference comparing the performance of NN and AR models, produced by TSNN2 and TSAR1 and TSAR2 methods. In the case of AR the MSE doesn't exceed the 1 MHz for both Athens and Pruhonice, while the NN model gives a MSE larger than 4 MHz in Athens and close to 3 MHz in Pruhonice. Concerning the seasonal dependence of the methods' performance, the AR models present a consistent pattern with maximum in the MSE during the summer and minimum in winter for both Athens and Pruhonice, although the pattern appears milder for Pruhonice. This indicates probably a dependence of the model prediction on the automatic scaling performance which during summer presents the maximum error due to frequent sporadic E layer or spread F occurrence, which is more intense over Athens. The seasonal pattern of the MSE obtained using the TSNN2 method presents noticeable differences, with a minimum in winter but only for prediction horizon greater than 3 h.

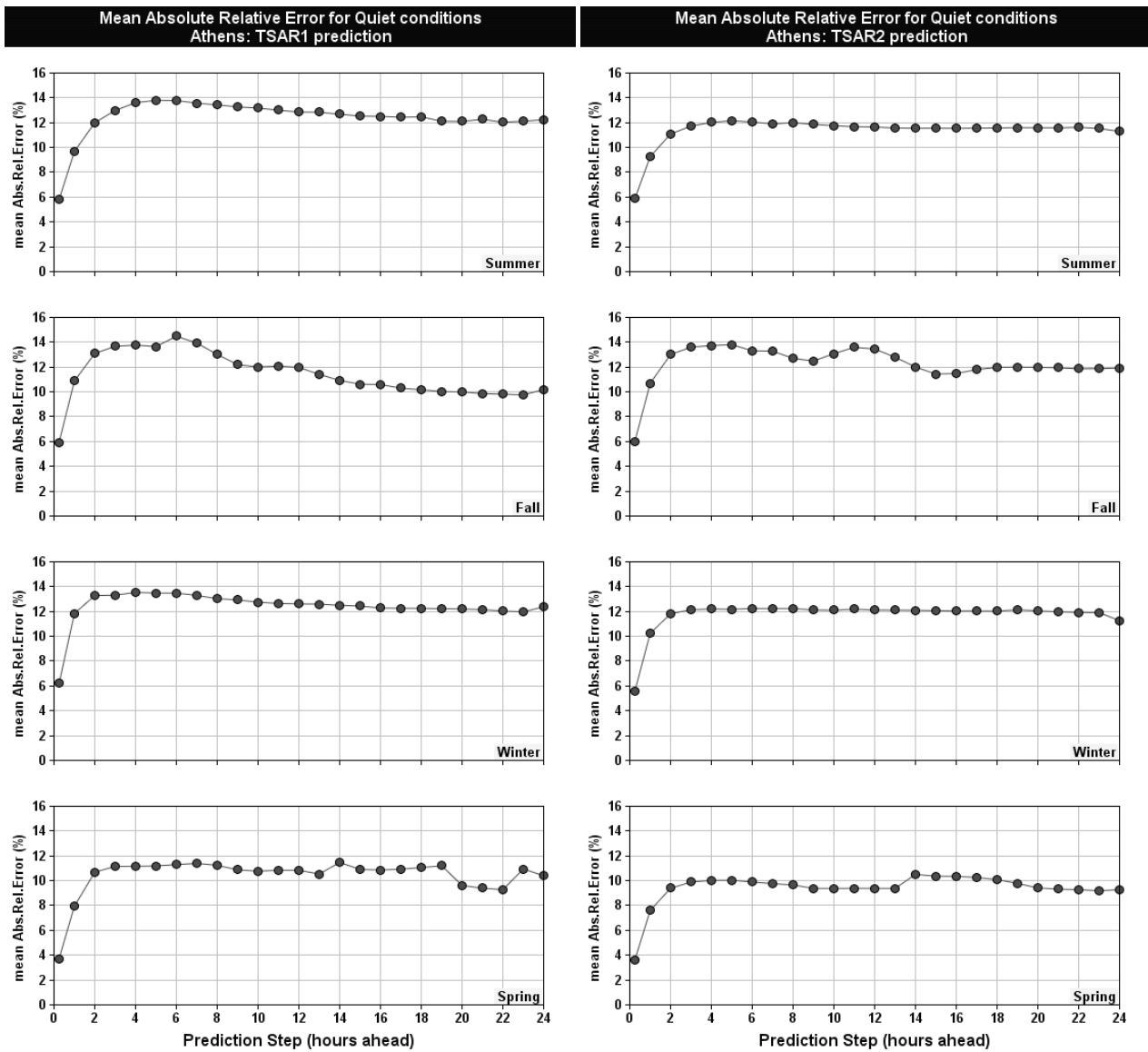


Fig. 9. The mean absolute relative error estimates for Athens as a function of the prediction step (1–24 h ahead) for each season.

To explore the reliability of TSAR1 and TSAR2 predictions in ionospheric forecasting from 1 to 24 h ahead, the mean absolute relative error as a function of the prediction time horizon is shown in Fig. 9 for Athens and in Fig. 10 for Pruhonice locations. The methods’ response shows a consistent pattern for both Athens and Pruhonice. The relative error gets relatively small values (4–6 %) for predictions 15 min ahead and reaches a maximum value of about 14% for predictions 4 or 5 h ahead, which in general is maintained and in some cases is decreased for predictions up to 24 h ahead. This pattern indicates that TSAR method provide statistically reliable ionospheric predictions up to 24 h ahead and could be considered as robust forecasting technique for the middle latitude ionosphere.

4 Summary and conclusions

In this paper a new method (TSAR1), designed to deliver short term forecasts (from 15 min up to 24 h) of the *foF2* parameter at middle latitudes has been presented. It is based on AR models and it has been implemented on line to work with real-time data in DIAS system. The method uses data from one calendar month to estimate the best AR model for the next calendar month according to MSE criterion. The method’s performance was also evaluated during both geomagnetically quiet and storm conditions for two middle latitude ionospheric locations, Athens and Pruhonice. For comparison purposes, the performance of a similar method, that instead of AR model it utilizes neural network models, the

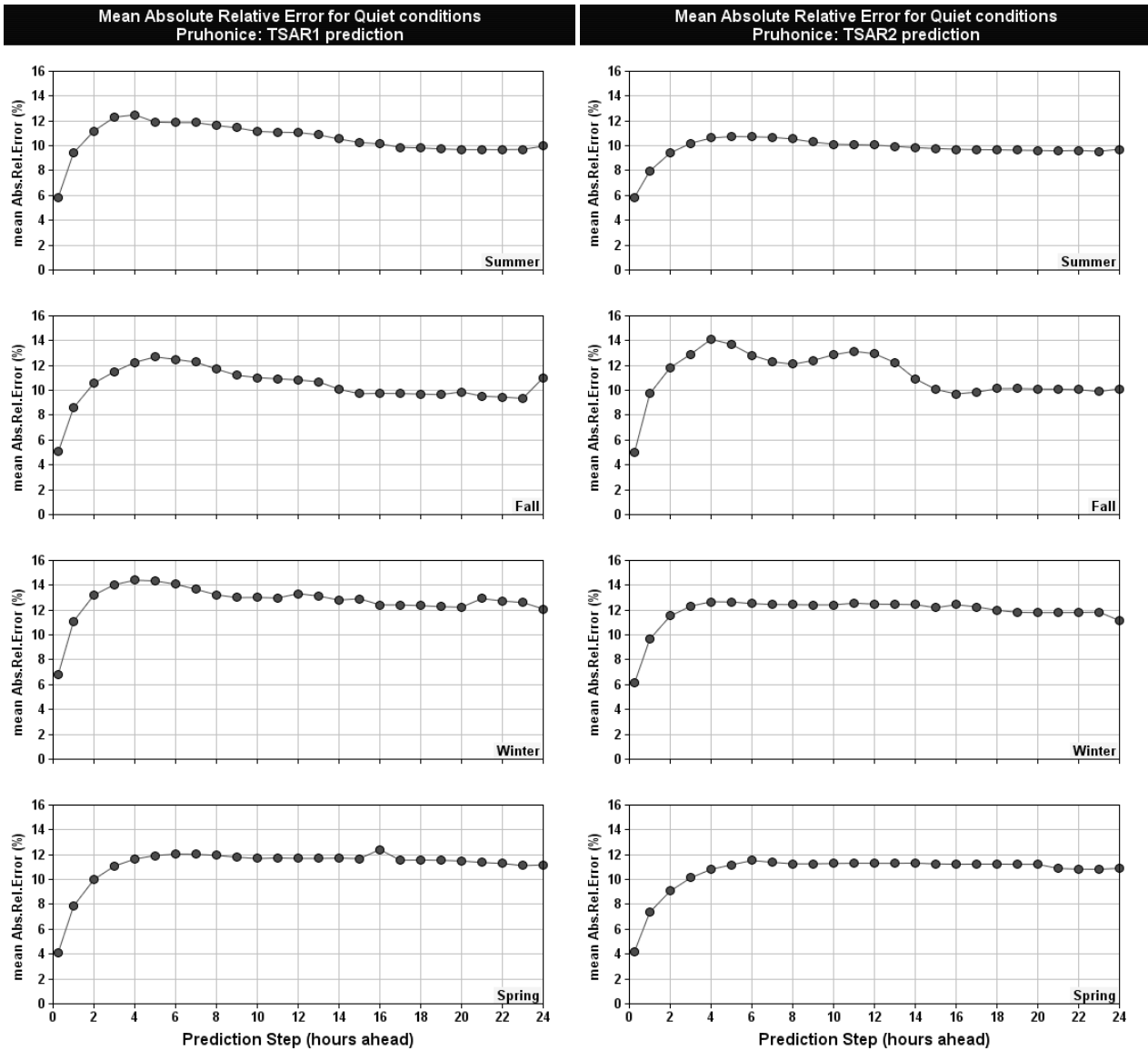


Fig. 10. The same as Fig. 9 for Pruhonice.

TSNN2, was also considered in our analysis. The TSNN2 uses two months of data for training and testing and for the fair evaluation of the relative performance of the two methods, the TSAR2 method was also considered in our tests. TSAR2 is the same as TSAR1 except that for the estimation of the new AR model at the beginning of each calendar month, the data of the last two calendar months are taken into account.

The comparison between the predictions obtained from the TSAR and TSNN methods during the same time intervals provided us the chance to investigate the efficiency of the linear modelling approach that TSAR method adopts in the prediction of f_oF2 parameter versus the non linear assumptions

assumed by TSNN2. Indeed, the deviations of the TSNN2 predictions from the observed values were higher compared to the corresponding ones obtained from both TSAR1 and TSAR2 predictions, either during storms or during quiet conditions for both Athens and Pruhonice locations. Moreover, TSNN2 method proved not very capable in capturing rapid changes in ionospheric response resulting by fast changing geospace environment conditions. The TSNN2 predictions seem also to be the most affected one by the recent ionospheric conditions and when an ionospheric disturbance is in progress, systematic deviations are reproduced in the method's estimations. All the above indicates that according to our results the ionospheric response is better modeled

using a linear model. This may be attributed to the following two reasons: i) the AR models are more capable in following the general periodic pattern of f_oF2 , and ii) the adopted FNN may not be the most proper one for the present application. There may be other FNNs with better performance than the selected one⁵, but since the number of all possible FNNs is huge, no exhaustive search can be performed to see if there exists indeed a better FNN.

Concerning the performance of TSAR1 and TSAR2, the comparative analysis gave evidence for consistency between TSAR1 and TSAR2 predictions, since the two methods provide qualitatively and quantitative similar results in all cases for both Athens and Pruhonice. In particular, during storm conditions the AR models appear to be sensitive in capturing successive changes from positive to negative (and vice versa) ionospheric storm phases. In respect to the storm development, the mean absolute relative error is rather small during the initial phase of the storm, with a general tendency to increase (up to about 30% in Athens and 40% in Pruhonice for predictions obtained six hours ahead) as the storm evolves and recovers. This is rather expected since the methods' predictions are based on the most recent measurements, which progressively include more and more disturbed data as we move to the end of the storm. The relative performance of the two methods (TSAR1 and TSAR2) during the storms presents slight differences sometimes in favor of TSAR1 and sometimes in favor of TSAR2. Therefore, one can argue that the longer training period doesn't necessarily improve the method's performance and since the differences are rather small (about 5% in the mean absolute relative error) TSAR1, which uses the smaller training data set, may be considered to be the most suitable for real time applications. It is also clear that the performance of TSAR method is not significantly affected by the properties of the training period in terms of the geomagnetic activity, since it provides predictions of statistically significant accuracy in all cases. This is very important for the real-time implementation of the method, since in real-time mode the training period could not be always the optimum one.

During quiet conditions the average MSE doesn't exceed the 1 MHz in both locations and for all cases. The relative error gets relatively small values (4–6 %) for predictions 15 min ahead and reaches a maximum value of about 14% for predictions 4 or 5 h ahead, which in general is maintained and in some cases is decreased for predictions up to 24 h ahead. This pattern indicates that TSAR method provides statistically reliable ionospheric predictions up to 24 h ahead.

According to our findings, TSAR1 method implemented on line in DIAS system provides very successful results for predictions 15 min and 1 h ahead and statistically reliable results for predictions up to 24 h ahead. This makes TSAR1

a powerful tool for interpolation purposes towards the development of reliable near real-time products and services of ionospheric specification, as well as a robust forecasting technique for the delivery of reliable forecasts for the middle latitude ionosphere, serving successfully the objectives of the DIAS system.

To conclude we have to notify the significant improvement in the prediction results using linear models for simulating the ionospheric response. Although more experiments with the method that employs neural networks (with larger data set, different number of inputs etc.) remain to be made, this result provides fresh insight in the current understanding for ionospheric forecasting modelling and might efficiently contribute to the development of reliable and accurate ionospheric specification tools, based on real-time networks of ionospheric sounders.

Acknowledgements. A preliminary version of this work was presented in the third European Space Weather Week as a contribution to the COST724 Action. Part of this work was funded by the DIAS project, sponsored by the eContent programme of the European Commission. The ionospheric observations from Pruhonice Digisonde were provided by the Ionospheric Group of Institute of Atmospheric Physics, Academy of Sciences of Czech Republic. The authors are grateful to T. Herekakis for his contribution to the experiments as well as to I. Kutiev and J. Goodman for constructive comments on the manuscript.

Topical Editor M. Pinnock thanks J. Goodman and I. Kutiev for their help in evaluating this paper.

References

- Belehaki, A. and Tsagouri, I.: On the occurrence of storm-induced nighttime ionisation enhancements at ionospheric middle latitudes, *J. Geophys. Res.*, 107, 121, doi:10.1029/2001JA005029, 2002.
- Belehaki, A., Cander, L. R., Zolesi, B., Bremer, J., Juren, C., Stanislawski, I., Dialektis, D., and Hatzopoulos, M.: DIAS project: The establishment of a European digital upper atmosphere server, *J. Atmos. Sol.-Terr. Phys.*, 67(12), 1092–1099, 2005.
- Belehaki, A., Cander, L. R., Zolesi, B., Bremer, J., Juren, C., Stanislawski, I., Dialektis, D., and Hatzopoulos, M.: Monitoring and forecasting the ionosphere over Europe: The DIAS project, *Space Weather*, 4, S12002, doi:10.1029/2006SW000270, 2006.
- Cander, L. R.: Toward forecasting and mapping ionospheric space weather under the COST actions, *Adv. Space Res.*, 31(4), 957–964, 2003.
- Crowley, G., Schoendorf, J., Roble, G., and Marcos, F. A.: Cellular structures in the high-latitude thermosphere, *J. Geophys. Res.*, 101, 211–224, 1996.
- Daniell Jr., R. E., Brown, L. D., Anderson, D. N., Fox, M. W., Doherty, P. H., Decker, D. T., Sojka, J. J., and Schunk, R. W.: Parameterized ionospheric model: A global ionospheric parameterization based on first principle models, *Radio Sci.*, 30(5), 1499–1510, 1995.
- Fuller-Rowell, T. J., Codrescu, M. V., and Wilkinson P.: Quantitative modeling of the ionospheric response to geomagnetic activity, *Ann. Geophys.*, 18 766–781, 2000a.

⁵If, for example, additional data or transformed versions of the data are given as input to the FNN.

- Fuller-Rowell, T. J., Araujo-Pradere, E., and Codrescu, M. V.: An empirical ionospheric storm-time correction model, *Adv. Space Res.*, 25(1), 139–146, 2000b.
- Fuller-Rowell, T. J., Millward, G. H., Richmond, A. D., and Codrescu, M. V.: Storm-time changes in the upper atmosphere at low latitudes, *J. Atmos. Sol.-Terr. Phys.*, 64(12–14), 1383–1391, 2002.
- Galkin, I. A., Khmyrov, G. M., Kozlov, A., et al.: Ionosonde networking, databasing, and Web serving, *Radio Sci.*, 41(5), RS5533, doi:10.1029/2005RS003384, 2006.
- Goodman, J. M.: Operational communication systems and relationships to the ionosphere and space weather, *Adv. Space Res.*, 36, 2241–2252, 2005.
- Kalouptsidis, N.: *Signal Processing Systems*, New York, John Wiley & sons, 1997.
- Koutroumbas, K. and Belehaki, A.: One-step ahead prediction of foF2 using time series forecasting techniques, *Ann. Geophys.*, 23, 3035–3042, 2005, <http://www.ann-geophys.net/23/3035/2005/>.
- Kutiev, I. and Muhtarov, P.: Modeling of midlatitude F region response to geomagnetic activity, *J. Geophys. Res.*, 106(A8), 15 501–15 509, 2001.
- Kutiev, I. and Muhtarov P.: Empirical modeling of global ionospheric foF(2) response to geomagnetic activity, *J. Geophys. Res.*, 108(A1), 1021, doi:10.1029/2001JA009134, 2003.
- McKinnell, L. A. and Poole, A. W. V.: Ionospheric variability and electron density profile studies with neural networks, *Adv. Space Res.*, 27(1), 83–90, 2001.
- Mikhailov, A. V., Depuev, V. H., and Depueva, A. H.: Short-term foF2 forecast: Present day state of art, in *Space Weather: Research towards applications in Europe*, Astrophysics and Space Science Library, 344, Springer, 169–184, 2007.
- Muhtarov, P. and Kutiev, I.: Autocorrelation method for temporal interpolation and short-term prediction of ionospheric data, *Radio Sci.*, 34(2), 459–464, 1999.
- Muhtarov, P., Kutiev, I., and Cander, L.: Geomagnetically correlated autoregression model for short-term prediction of ionospheric parameters, *Inverse Problems*, 18, 49–65, 2002.
- Stanislawska I. and Zbyszynski, Z.: Forecasting of the ionospheric quiet and disturbed foF2 values at a single location, *Radio Sci.*, 36(5), 1065–1071, 2001.
- Stanislawska, I. and Zbyszynski, Z.: Forecasting of the ionospheric characteristics during quiet and disturbed conditions, *Ann. Geophys.*, 45(1), 169–175, 2002.
- Tsapouri, I. and Belehaki, A.: A new empirical model of middle latitude ionospheric response for space weather applications, *Adv. Space Res.*, 37, 420–425, 2006.
- Tulunay, Y., Tulunay, E., and Senalp, E. T.: The neural network technique -1: a general exposition, *Adv. Space Res.*, 33, 983–987, 2004a.
- Tulunay, Y., Tulunay, E., and Senalp, E. T.: The neural network technique – 2: an ionospheric example illustrating its application, *Adv. Space Res.*, 33, 988–992, 2004b.
- Wintoft, P. and Cander, L. R.: Twenty-four hour predictions of foF2 using time delay neural networks, *Radio Sci.*, 35, 2, 395–408, 2000a.
- Wintoft, P. and Cander L.: Ionospheric foF2 storm forecasting using neural networks, *Phys. Chem. Earth*, 25(2), 267–273, 2000b.